Improved strategies for DNP-enhanced 2D ^{1}H-X heteronuclear correlation spectroscopy of surfaces

Takeshi Kobayashi,[a] Frédéric A. Perras,[a] Umesh Chaudhary,[b] Igor I. Slowing,[a,b] Wenyu, Huang,[a,b] Aaron D. Sadow[a,b] and Marek Pruski[a,b,]*

[a]Ames Laboratory, U.S. Department of Energy, Ames, Iowa, 50011, U.S.A.

[b]Department of Chemistry, Iowa State University, Iowa 50011, U.S.A.

KEYWORDS Dynamic Nuclear Polarization, Solid-State NMR, Heteronuclear Correlation, Catalysis, Surface Science.

Abstract

We demonstrate that the dynamic nuclear polarization (DNP)-enhanced ^{1}H-X heteronuclear correlation (HETCOR) measurements of surface species are better accomplished by using proton-free solvents. This approach notably prevents HETCOR spectra from being obfuscated by the solvent-derived signals otherwise present in DNP measurements. Additionally, in the hydrogen-rich materials studied here, which included functionalized mesoporous silica nanoparticles and metal organic frameworks, the use of proton-free solvents afforded higher sensitivity gains than the commonly used solvents containing protons. We also explored the possibility of using a solvent-free sample formulation and the feasibility of indirect detection in DNP-enhanced HETCOR experiments.

Highlights

- DNP-enhanced 2D ^{1}H-X HETCOR spectra of surface species were measured using proton-free solvents.
- The approach eliminates solvent-derived correlation signals.
- In hydrogen-rich materials, the use of proton-less solvents improves the DNP performance.

1. Introduction

The inherently low sensitivity of solid-state nuclear magnetic resonance (SSNMR) spectroscopy often prevents the detection of nuclei with low gyromagnetic ratio (γ) and/or low natural isotopic abundance, such as ^{13}C and ^{15}N. The sensitivity woes are particularly challenging in structural determinations involving measurements of two-dimensional (2D) heteronuclear correlation (HETCOR) spectra. In solution-state NMR, an indirect detection of low-γ nuclei via high-γ nuclei, in the HMQC and HSQC experiments,[1, 2] has been long used to improve the sensitivity of HETCOR spectroscopy. The advent of fast magic-angle spinning (MAS) enabled the introduction of similar concepts to SSNMR, with the so-called indirectly-detected HETCOR (idHETCOR) experiment.[3, 4] The significant sensitivity enhancement afforded by idHETCOR widened the practical applications of 2D correlation spectroscopy in natural abundance solids[5-7] and, in some cases, also enabled the observation of 2D spectra of surface species.[4, 8] Further sensitivity gains are, however, required for examining small surfaces, minute concentrations of species, or insensitive nuclei.

Dramatic sensitivity gains in NMR spectroscopy can be now provided by dynamic nuclear polarization (DNP), which relies on irradiating paramagnetic dopants near their electron Larmor frequency and subsequently transferring their magnetization to the nuclei. DNP offers potential sensitivity gains of γ_e/γ_n, which corresponds to, for example, ~6500 for ^{15}N, when compared to conventional NMR techniques.[9-11] The last two decades have seen a series of breakthroughs including advances in gyrotron technology[12, 13] and cryogenic magic angle spinning (MAS),[14-16] as well as the introduction and systematic improvement of exogenous sources of unpaired electrons (such as biradical polarizing agents),[17-21] which have together enabled the extension of DNP-enhanced NMR spectroscopy to ever higher magnetic field strengths.[22] These developments have provided a new, much needed, approach for the characterization of

challenging solids. In particular, the DNP-enabled, multidimensional correlation NMR experiments can yield unprecedented structural and conformational details about the surface-bound species.[23-29]

In modern high-field DNP SSNMR, solvents are used to disperse the biradical polarization agents within the sample. The solvent can also facilitate the transport of hyperpolarized magnetization from the radical source to the bulk of the observed nuclei by ^{1}H-^{1}H spin diffusion. Unfortunately, the NMR signals from the solvent itself, and their correlations to the sample, appear in the ^{1}H-X HETCOR spectra, often obscuring the signals of interest and hampering the signal assignment.[23, 24] An optimization of experimental parameters can suppress the solvent-sample correlation signals, often at the expense of sensitivity. Indeed, Yarava et al. successfully mitigated the solvent-derived signal by using a short cross-polarization contact time.[30] They also filtered out fast-relaxing solvent signals from slow-relaxing signals of a microcrystalline L-histidine sample by inserting a spin lock precedent to a contact pulse. The suppression of solvent ^{1}H signals even enabled the acquisition of a DNP-enhanced high-resolution ^{1}H-^{1}H correlation spectrum. This approach, however, requires that there is a sizeable difference in relaxation times between the solvent and the sample, which is often not the case in non-crystalline samples in which the sites on interest are located on the surface in intimate contact with the solvent. An alternative approach to solvent suppression was recently presented by Lee et al. who used ^{2}H-^{13}C dipolar recoupling in order to selectively attenuate the signals from deuterated glycerol found in the "DNP juice" of importance in biological DNP-MAS NMR.[31] A careful choice of solvent can also minimize signal overlap, leading to a higher discrimination of the solvent-derived signals;[32] however, this approach requires a prior knowledge of the spectrum and can be impractical for the characterization of unknown samples.

The use of fully deuterated solvents, which is common in solution NMR, represents a desirable approach, provided that (i) there is no H/D isotope exchange upon the use of deuterated solvents and (ii) the material itself possesses a sufficiently high inherent proton population to hyperpolarize the distant nuclei of interest via spin diffusion. In earlier DNP studies, partially deuterated solvents were shown to lead to the highest enhancements.[33-36] Furthermore, Le et al. reported that the use of a fully deuterated solvent (1,1,2,2-tetrachloroethane-d_2, TCE-d_2) did not result in the decrease of sensitivity enhancement for the ^{13}C signals from microporous polymers.[37]

Another promising approach for the removal of signals from the solvent is to simply use none. For example, Takahashi et al. reported that a sample impregnated with a radical solution and subsequently dried under vacuum, offered a reasonable enhancement for the ^{13}C signals of a protein.[38] In that case, however, the addition of glucose was needed to prevent the aggregation of radical molecules; leading once again to the presence of unwanted signals in the spectra.

Herein, we explore the feasibility of acquiring clean DNP-enhanced ^{1}H-X (X = ^{13}C and ^{15}N) HETCOR spectra of surface-bound species at natural abundance, by using protonless solvents or no solvent at all. Two model systems were chosen for this investigation: mesoporous silica nanoparticles functionalized with 3-(3-phenylureido)propyl groups (PUP-MSNs) and UiO-66-type metal organic frameworks (MOFs) containing Pt^{2+} ions (Pt/UiO-66-NH_2, see the Supporting Information for synthesis details). The pores of the MSNs are sufficiently wide (~3.7 nm) to allow for penetration of the biradicals into the nanoparticles, whereas in the case of MOFs the magnetization can be only transported within the nanoparticles via ^{1}H-^{1}H spin diffusion (Fig. 1). In both cases, the pores are sufficiently large to allow them to become filled by the solvent. We

also explored the feasibility of combining DNP with the idHETCOR experiment to further improve sensitivity.

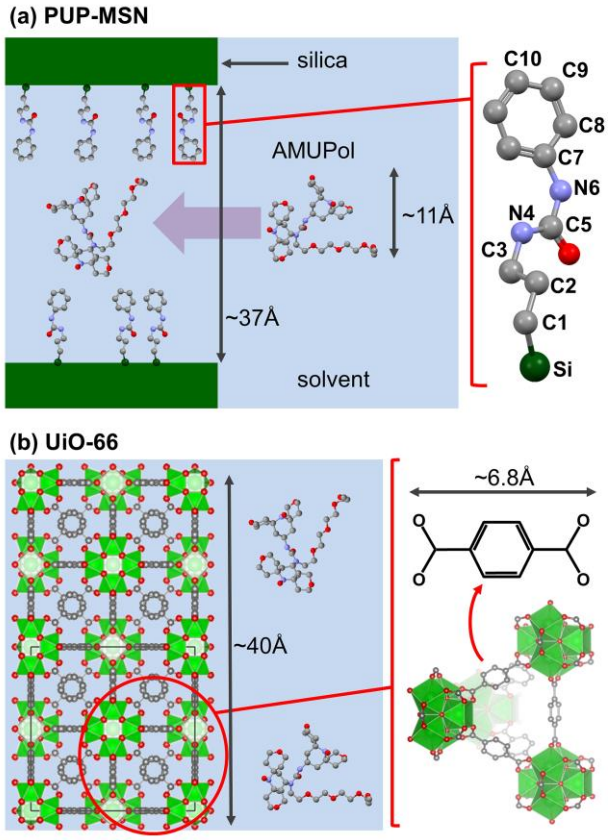

Fig. 1. Schematic sketches of (a) PUP-MSN and (b) UiO-66 MOF impregnated with 10 mM aqueous solution of AMUPol. The figures accurately reflect the relative sizes of pores and molecules; note that AMUPol cannot penetrate into the MOFs. Hydrogen atoms are omitted for clarity.

2. Experimental

2.1. Samples Preparation.

2.1.1. PUP-MSNs.

PUP-MSNs were synthesized using a previously reported co-condensation method.[28, 39] The surfactant was extracted by refluxing methanol in a Soxhlet extractor for 3 days. After drying under vacuum at room temperature, the resulting product had the surface area = 519 m^2/g, pore volume = 0.59 cm^3/g, and a narrow pore size distribution centered at 3.7 nm. Further details about the synthesis and material characterizations are described elsewhere.[28, 39]

2.2.2. UiO-66-NH_2 and Pt/UiO-66-NH_2.

UiO-66-NH_2 MOF was synthesized and purified as reported previously.[40, 41] Pt was loaded by suspending the UiO-66-NH_2 in an aqueous solution of K_2PtCl_4 for 20 h. The solid product was separated by centrifugation, then washed with water, and dried under vacuum at 120 °C for 8 h (Pt/UiO-66-NH_2). Further details were reported in our earlier study.[41]

2.2.3. Solid-state NMR experiments

The DNP-enhanced measurements were performed on a Bruker BioSpin DNP NMR spectrometer, operated at 9.4 T (400 MHz), equipped with a gyrotron generating microwave (MW) irradiation at 264 GHz. The experiments included one-dimensional cross-polarization magic angle spinning (CPMAS) spectra of ^{13}C and ^{15}N (denoted as $^{13}C\{^1H\}$ and $^{15}N\{^1H\}$ CPMAS), as well as two-dimensional (2D) through-space HETCOR spectra, detected via low-gamma nuclei (denoted at $^{13}C\{^1H\}$ and $^{15}N\{^1H\}$ HETCOR) or ^1H nuclei ($^1H\{^{15}N\}$ idHETCOR, where 'id' denotes indirect detection). A conventional 2D $^1H\{^{13}C\}$ idHETCOR[4] spectrum was also measured using a Varian NMR System 600 spectrometer, operated at 14.1 T and equipped with a FastMAS^{TM} 1.6-mm probe. The experimental parameters are given in the figure captions, where ν_R is the MAS rate, τ_{CP} is the CP contact time, and τ_{RD} is the recycle delay. The NMR chemical shifts are referenced to TMS (^1H and ^{13}C) and ammonia (^{15}N).

For the DNP measurements, samples were impregnated with 10 mM AMUPol[20] dissolved in water (H_2O, D_2O:H_2O (9:1), and D_2O) or DMSO (DMSO, DMSO-d_6/DMSO (9:1), and DMSO-d_6), packed in 3.2-mm sapphire rotors and spun at a temperature of ~100 K. The DMSO was tested in the context of ^{1}H-^{15}N HETCOR measurements, to prevent potential deuteration of the NH moieties of the PUP groups via H/D isotope exchange. Solvents deuterated to 90% were tried as this is a common deuteration level used for DNP SSNMR measurements in biological systems. The 'solvent-less' sample formulation involved impregnation of the PUP-MSN powder with a 10 mM AMUPol solution in H_2O followed by dehydration under vacuum at room temperature. Lastly, the popular 16 mM solution of TEKPol[25] in TCE used in materials science was trialed using fully deuterated, or protonated TCE. The samples are listed in Table 1 and will be referred in the following as samples 1-9.

3. Results and Discussion

Prior to the acquisition of 2D HETCOR spectra, we assessed the possible sensitivity penalty that might be imposed on the DNP measurements by the departure from proton-containing solvents as a result of diminished spin diffusion or changes in DNP build-up times. To this end, we acquired the $^{13}C\{^{1}H\}$ CPMAS and $^{29}Si\{^{1}H\}$ CPMAS spectra of PUP-MSNs and MOFs to measure the DNP enhancement factor ε, defined as the ratio of the signal intensities per scan obtained with and without the microwave irradiation, as well as the relative sensitivity per unit of time $(\varepsilon)^2/\tau_{DNP}$, where τ_{DNP} is the DNP build-up time, for several sample formulations.

The ε and $(\varepsilon)^2/\tau_{DNP}$ values measured from the $^{13}C\{^{1}H\}$ CPMAS spectra of PUP-MSNs are listed in Table 1. Notably, the use of fully deuterated solvents did not inflict any noteworthy sensitivity penalty. In fact, fully deuterated solvents provided higher ε values than protonated solvents (by 82% for water and 42% for DMSO), whereas the sensitivity per unit of time

remained almost unchanged after taking into account the increased τ_{DNP} time. We also note that the $^{15}N\{^1H\}$ CPMAS experiment on PUP-MSN with DMSO-d_6 yielded a ^{15}N spectrum of naturally abundant surface species within just a few min (Fig. S1 in Supporting Information). A notable exception appears to be the TCE formulations for which solvent deuteration provided a slightly lower sensitivity. In this case, however, the lack of τ_{DNP} lengthening upon deuteration suggests that the DNP process is limited by the T_1 of the functional groups. Indeed, repeating the same experiment on a bare MSN yielded nearly-identical sensitivities for both sample formulations.

Table 1. DNP performance for PUP-MSNs prepared using different solvents.

sample	solvent	τ_{DNP} [a] (s)	ε [b]	ε^2/τ_{DNP} (s^{-1})
1 [c]	H_2O	2.3	40	696
2 [c]	D_2O:H_2O (9:1)	6.3	61	591
3 [c]	D_2O	7.8	73	683
4 [c]	DMSO	2.0	22	242
5 [c]	DMSO-d_6:DMSO (9:1)	5.0	24	115
6 [c]	DMSO-d_6	5.4	34	214
7 [c]	solvent-less	5.4	8	12
8 [d]	TCE	6.1	80	1049
9 [d]	TCE-d_2	6.8	65	621

[a] The DNP build-up curve for the samples prepared using water as a solvent is biexponential; the number in the table is the average build-up time. [b] The ε values were based on the intensities of $^{13}C\{^1H\}$ CPMAS spectra, except for the solvent-less sample, where it was based on ^1H and $^{29}Si\{^1H\}$ CPMAS spectra. [c] These solutions were prepared with the AMUPol biradical in a 10 mM concentration. [d] These solutions were prepared with the TEKPol biradical in 16 mM concentrations.

The improvement of sensitivity upon partial deuteration of solvents in biological systems has been attributed to the reduction in the number of nuclei to polarize, while reductions in T_1

relaxation and spin diffusion rates of the ^{1}H nuclei can be detrimental; obtaining a proper balance between the two is generally important.[17, 33, 34] In the case of the PUP-MSNs used in this study, if we assume that the pores are filled with D_2O:H_2O (90:10 v/v), a common deuteration level used in biological DNP, the solvent supplies a proton concentration of ~7 mmol/g, which amounts to only about 20% of protons within the pores (~28 mmol/g of protons is provided by the PUP and silanol groups, see Supporting Information for details). Additionally, as already mentioned, the pores of PUP-MSNs are large enough to accommodate the AMUPol molecule and thus long-range spin diffusion is not needed. Consequently, the sample itself provides sufficient proton concentration to mediate spin diffusion to the observed nuclei.

To demonstrate the impact of solvent protons on the quality of 2D HETCOR spectra, we measured the DNP-enhanced ^{13}C{^{1}H} and ^{15}N{^{1}H} HETCOR spectra of PUP-MSNs (samples 1-3 in Table 1). As can be seen in Fig. 2a-c, the ^{13}C projections of these spectra are very similar, notwithstanding the small differences in relative peak intensities. However, the observed cross-peak patterns and ^{1}H chemical shifts differ considerably. Notably, the spectrum measured using H_2O (sample 1, Fig. 2a), is dominated by solvent-related correlations. In spite of using ^{1}H-^{1}H decoupling, all correlation signals are similarly elongated along the ^{1}H dimension, featuring a narrower common cross-peak with maximum centered at around δ_H ~ 8 ppm and a broad underlying base, which extends to around 1 ppm. Although the resonance at 8 ppm matches the chemical shift of aromatic protons in PUP, here we attribute it largely to ^{1}H nuclei in amorphous ice, whose chemical shift was reported in the same range and was further verified by the ^{1}H NMR spectrum of PUP-MSN with AMUPol in 100% H_2O (dashed line in Fig. 2a).[42, 43] This interpretation also accounts for the fact that these nuclei exhibit dominant cross-peaks with

carbons C1, C2 and C3 in PUP (Fig. 2a). The broad base is ascribed to ^{1}H nuclei in the network of hydrogen-bonded silanol protons and the first monolayer of hydrogen-bonded water.[43, 44]

With the decrease of H_2O content in the solution, the resolution in the ^{1}H dimension was improved and the correlation signals involving ^{1}H spins in PUP became clearly identifiable. In the spectrum obtained with 100% D_2O as a solvent (Fig. 2c), only the cross-peaks representing the PUP moieties are present. In comparing this spectrum to one taken using the idHETCOR method on a conventional spectrometer at room temperature under 32 kHz MAS (Fig. 1d), several points may be noted. Firstly, despite the use of frequency switched Lee-Goldburg (FLSG) ^{1}H-^{1}H homonuclear decoupling[45] during the ^{1}H evolution period, the ^{1}H line widths observed at 100 K are broader. Notwithstanding this broadening, however, the signal-to-noise ratio of the DNP-enhanced spectrum (acquired >6 times faster) is much higher. Lastly, the ^{1}H chemical shifts of aliphatic protons in PUP are strongly influenced by temperature, most likely due to the change of PUP conformation.

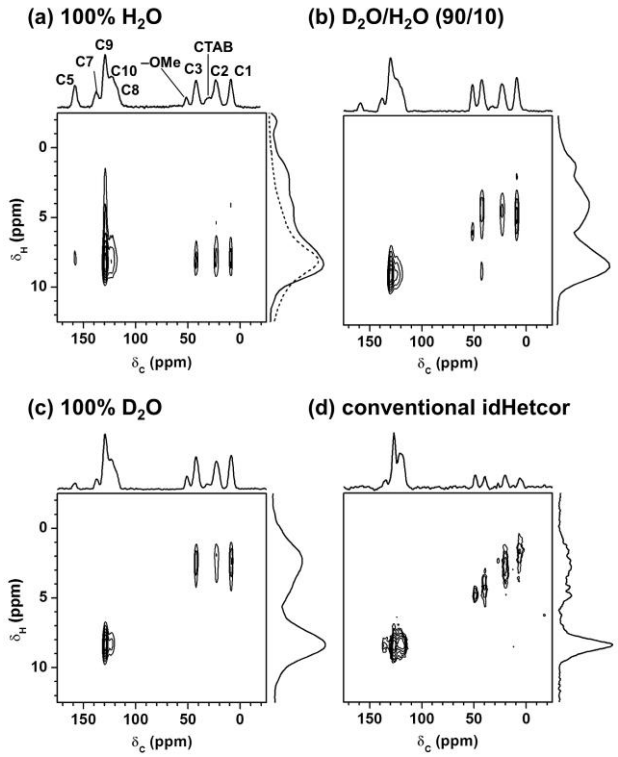

Fig. 2. DNP-enhanced $^{13}C\{^{1}H\}$ HETCOR spectra of PUP-MSNs impregnated with 10 mM aqueous solution of AMUPol (samples 1-3, Table 1) (a-c), and conventional $^{1}H\{^{13}C\}$ idHETCOR spectrum of PUP-MSN (d). Spectra (a-c) were recorded at 100 K with ν_R = 8 kHz; τ_{CP} = 1 ms; τ_{RD} = 3 s (a), 8 s (b) and 10 s (c); FSLG ^{1}H-^{1}H homonuclear decoupling[45] during t_1; heteronuclear SPINAL-64[46] decoupling during t_2; and total acquisition times of 13 min (a), 34 min (b), and 43 min (c). The same floor level was applied to spectra a-c to facilitate comparison. Spectrum (d) was acquired at room temperature with ν_R = 32 kHz, τ_{CP} = 0.5 ms, τ_{RD} = 1 s, SPINAL-64[46] decoupling during t_1 (^{1}H) and t_2 (^{13}C), and total acquisition times of 4.5 h. In (a) a dashed line is used to show the 1D ^{1}H MAS spectrum of the same sample, which is dominated by the signals from ice.

The interferences from the solvents are also prominent in the ^{1}H-^{15}N HETCOR spectra of samples 1, 3 and 6, shown in Fig. 3a, b and c, respectively. We have previously reported an indirectly detected $^{1}H\{^{15}N\}$ spectrum of PUP-MSN taken on a conventional spectrometer,[7] which yielded two cross-peaks attributed to nitrogens N4 and N6 and their associated protons (we refer here to the PUP scheme shown in Fig. 1). For reference, in Fig. 3 we marked the positions of cross-peaks from this earlier study with asterisks. Note that the asterisks match well only with the spectrum obtained using DMSO-d_6 as a solvent (Fig. 3c). In the spectrum obtained with H_2O (sample 1, Fig. 3a), the dominant cross-peaks correlate nitrogens N4 and N6 with protons resonating at $\delta_H \sim 8$ ppm, attributed to protons in amorphous ice (*vide supra*). Sample 3, on the other hand, yielded a dominant signal between N4 and nearby methylene protons (Fig. 3b). The correlation signals at $\delta_H \sim 8$ ppm represent the aromatic protons in PUP, whereas the amide protons in NH moieties were significantly attenuated due to the H/D isotope exchange. A spectrum with no interference from the solvent was finally obtained by using aprotic deuterated

solvent, DMSO-d_6 (Fig. 3c), in which the ^{1}H-^{15}N correlation signals appeared in their proper positions.

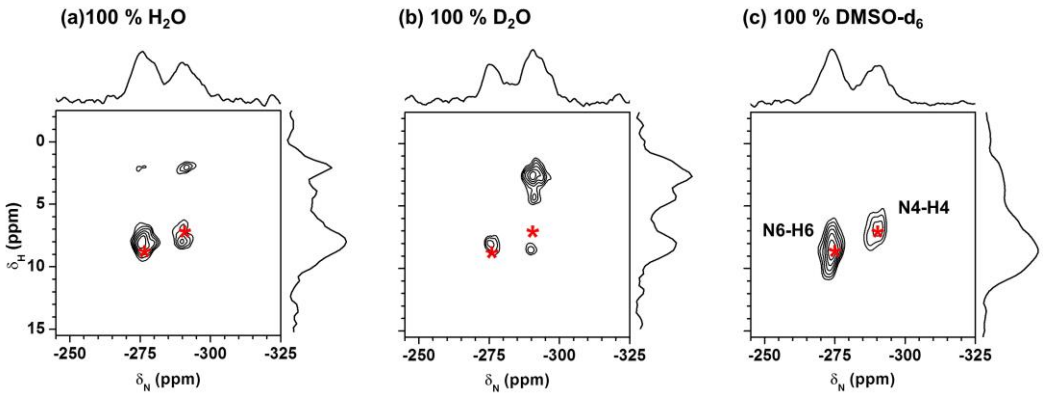

Fig. 3. DNP-enhanced $^{15}N\{^{1}H\}$ HETCOR spectra of PUP-MSNs: (a) sample 1, (b) sample 3, and (c) sample 6. The spectra were recorded with ν_R = 8 kHz; τ_{CP} = 1 ms; and τ_{RD} = 2.5 s (a), 10 s (b) and 7 s (c); and total acquisition times of 1.5 h (a), 5.7 h (b) and 4 h (c). FSLG ^{1}H-^{1}H homonuclear decoupling and heteronuclear SPINAL-64 decoupling were applied during t_1 and t_2, respectively.

To examine the practicality of using a solvent-free, or matrix-free, approach, we prepared an AMUPol-doped PUP-MSN by evaporating the solvent (H_2O) at room temperature under vacuum (sample 7). The DNP-enhanced $^{13}C\{^{1}H\}$ CPMAS spectrum of this sample showed an enhancement factor ε = 8 (Table 1). Perhaps higher enhancements can be achieved by optimizing the radical concentration. The most likely, albeit unconfirmed, cause of the lower DNP effect in this case is the agglomeration of biradicals within the pores due to their poor affinity to the surface. We note that we have not observed any quantifiable loss of intensity per scan in the spectrum of the solvent-free PUP-MSN acquired with the microwave irradiation turned off, when compared to samples with solvents, suggesting that there is no increased quenching.[47]

Note that the affinity of the polarizing agent to the sample of interest can be improved by using a "gluing agent" to better disperse the radicals in the dried sample, as indeed demonstrated in biomolecular systems by Takahashi et al.,[38] who reported an ε value of 10 in $^{13}C\{^{1}H\}$ CPMAS spectra of adenosine using TOTAPOL. However, such a strategy introduces new undesired resonances into the spectra.

To further test the utility of fully deuterated solvents, we acquired DNP-enhanced $^{13}C\{^{1}H\}$ and $^{15}N\{^{1}H\}$ spectra of UiO-66-NH_2 and Pt/UiO-66-NH_2 MOFs. In both samples, the pores are too small to accommodate the biradical molecules,[40] and thus the hyperpolarization has to be delivered to the bulk of the ca. 100 nm crystallites via ^{1}H-^{1}H spin diffusion by the intrinsic protons of the sample itself. In our earlier study of this system, we used a 10 mM solution of TOTAPOL in H_2O to acquire $^{15}N\{^{1}H\}$ DNP CPMAS spectra and demonstrated that Pt^{2+} coordinates with two NH_2 groups from the MOF and two Cl^- groups from the metal precursor in a square-planar arrangement.[41] Subsequent high-resolution ^{195}Pt experiments showed that some complexes are partially hydrolyzed.[48] Here, we first use $^{13}C\{^{1}H\}$ CPMAS to assess the effects of fully deuterated solvents by comparing the values of ε, τ_{DNP}, and $(\varepsilon)^2/\tau_{DNP}$ between the UiO-66-NH_2 with 100% DMSO and 100% DMSO-d_6 (Table 2). As expected, the observed ε values were lower than those for PUP-MSN (Table 1), because the signal enhancement in the bulk of UiO-66-NH_2 relies on the abovementioned 'remote excitation' by ^{1}H-^{1}H spin diffusion.[28,43] Surprisingly, the use of a fully deuterated solvent did not impose any sensitivity penalty, with the relative sensitivity per unit of time being even higher than in DMSO.

Table 2. DNP performance for UiO-66-NH_2 with AMUPol dissolved in DMSO and DMSO-d_6.[a]

solvent	τ_{DNP} (s)	ε	ε^2/τ_{DNP} (s^-

			^{1})
DMSO	1.9	7	26
DMSO-d_6	2.6	10	38

[a] The parameters were estimated from $^{13}C\{^{1}H\}$ CPMAS spectra, in the same manner as those reported in Table 1.

The DNP-enhanced 2D $^{15}N\{^{1}H\}$ HETCOR spectra of UiO-66-NH_2 and Pt/UiO-66-NH_2 MOFs measured using DMSO-d_6 are shown in Fig. 4. The spectra exhibit 'clean' ^{15}N-^{1}H cross peaks, with no interference from the solvent, which are straightforwardly assigned to NH_2 and $NH_2\cdots Pt^{2+}$ moieties.[41] The HETCOR experiment also interestingly revealed a ~1 ppm ^{1}H chemical shift increase upon coordination to Pt, consistent with previous $^{1}H\{^{195}Pt\}$ measurements. We do not report the DNP enhancement values for these spectra, because their acquisition without the microwave radiation is beyond the current capabilities of conventional SSNMR; however, they should be equivalent to those measured using ^{13}C NMR, see Table 2.

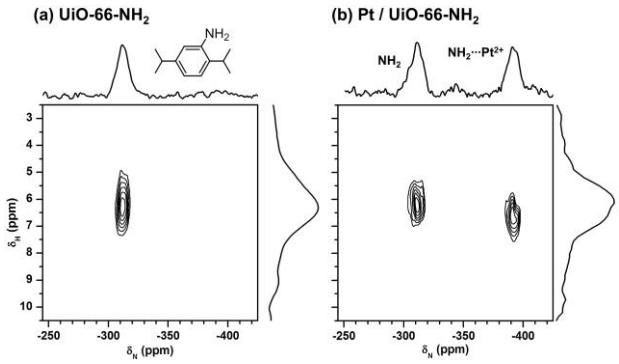

Fig. 4. DNP-enhanced $^{15}N\{^{1}H\}$ HETCOR spectra of (a) UiO-66-NH_2 and (b) Pt/UiO-66-NH_2. Both samples were impregnated with a 10 mM DMSO-d_6 solution of AMUPol. The spectra were acquired in 2 h and 50 min using ν_R = 10 kHz, τ_{CP} = 2 ms, and τ_{RD} = 10 s. FSLG ^{1}H-^{1}H homonuclear decoupling was used during the ^{1}H evolution period (t_1) and SPINAL-64 decoupling was employed during the acquisition period (t_2).

The absence of solvent protons invokes the possibility of combining the sensitivity advantage of DNP with ^{1}H-detection. Indeed, Yarava et al. demonstrated that the suppression of solvent signals enabled the acquisition of DNP-enhanced ^{1}H-^{1}H correlation spectra.[30] In Fig. 5, we show the DNP-enhanced ^{1}H{^{15}N} idHETCOR spectra of PUP-MSNs (sample 6) and UiO-66-NH_2, which were both obtained using the proton-free solvent (DMSO-d_6). As expected, the sensitivity is improved by the indirect detection scheme, by a factor of almost 2 in the case of sample 6, and by 40% in UiO-66-NH_2; however, the absence of ^{1}H-^{1}H homonuclear decoupling during the acquisition period resulted in very poor resolution in the ^{1}H dimension. Clearly, to realize the full benefit of DNP-enhanced indirect detection, the experiment must be performed under fast MAS.[49]

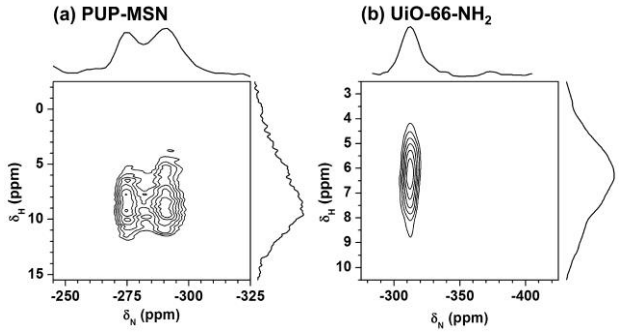

Fig. 5. DNP-enhanced ^{1}H{^{15}N} idHETCOR spectra of (a) PUP-MSNs (sample 6) and (b) UiO-66-NH_2. The samples were impregnated with 10 mM DMSO-d_6 solution of AMUPol. The spectra were acquired in 4 h (a) and 2 h 50 min (b), using ν_R = 10 kHz, τ_{CP} = 4 ms (a) and 2 ms (b), and τ_{RD} = 7 s (a) and 10 s (b). SPINAL-64 ^{1}H heteronuclear decoupling during t_1 and CW ^{15}N heteronuclear decoupling during t_2.

4. Summary

In summary, we have demonstrated that the use of proton-free solvents is a practical approach to eliminate the solvent-derived correlation signals from the DNP-enhanced HETCOR spectra of

materials. This methodology implies that there is no H/D isotope exchange with deuterated solvents and relies upon the sample's strongly coupled innate protons to mediate the spin diffusion and hyperpolarize the targeted spins on the surface or in the bulk. In samples where such networks of protons exist, the use of proton-free solvents yielded significantly improved 2D HETCOR spectra with no loss in sensitivity. The sensitivity of DNP-enhanced HETCOR experiments may be additionally improved by the application of a ^{1}H-detected scheme, especially if the resolution in the ^{1}H dimension can be improved by fast MAS.

ASSOCIATED CONTENT

Supporting Information.

Estimation of protons concentration in PUP-MSNs.

Corresponding Author

*Marek Pruski: Tel: (515)294-2017. E-mail: mpruski@iastate.edu

ACKNOWLEDGMENT

This research is supported by the U.S. Department of Energy (DOE), Office of Basic Energy Sciences, Division of Chemical Sciences, Geosciences, and Biosciences, and by the LDRD program at the Ames Laboratory (T.K., I.I.S., A.D.S., M.P.). Support for F.P. is through a Spedding Fellowship also funded by the LDRD program at the Ames Laboratory. The Ames Laboratory is operated for the U.S. DOE by Iowa State University under Contract No. DE-AC02-07CH11358. Support from Royalty Account and Iowa State University startup funds is

also acknowledged (W.H.). F. P. thanks NSERC and the government of Canada for a Banting postdoctoral fellowship.

REFERENCES

[1] L. Muller, Sensitivity enhanced detection of weak nuclei using heteronuclear multiple quantum coherence, J. Am. Chem. Soc. 101 (1979) 4481-4484.
[2] G. Bodenhausen, D.J. Ruben, Natural abundance N-15 NMR by enhanced heteronuclear spectroscopy, Chem. Phys. Lett. 69 (1980) 185-189.
[3] Y. Ishii, R. Tycko, Sensitivity enhancement in solid state N-15 NMR by indirect detection with high-speed magic angle spinning, J. Magn. Reson. 142 (2000) 199-204.
[4] J.W. Wiench, C.E. Bronnimann, V.S.-Y. Lin, M. Pruski, Chemical shift correlation NMR spectroscopy with indirect detection in fast rotating solids: Studies of organically functionalized mesoporous silicas, J. Am. Chem. Soc. 129 (2007) 12076-12077.
[5] D.H. Zhou, G. Shah, C. Mullen, D. Sandoz, C.M. Rienstra, Proton-detected solid-state NMR spectroscopy of natural-abundance peptide and protein pharmaceuticals, Angew. Chem. Int. Ed. 48 (2009) 1253-1256.
[6] G.P. Holland, B.R. Cherry, J.E. Jenkins, J.L. Yarger, Proton-detected heteronuclear single quantum correlation NMR spectroscopy in rigid solids with ultra-fast MAS, J. Magn. Reson. 202 (2010) 64-71.
[7] S.M. Althaus, K. Mao, J.A. Stringer, T. Kobayashi, M. Pruski, Indirectly detected heteronuclear correlation solid-state NMR spectroscopy of naturally abundant N-15 nuclei, Solid State Nucl. Magn. Reson. 57-58 (2014) 17-21.
[8] K. Mao, T. Kobayashi, J.W. Wiench, H.-T. Chen, C.-H. Tsai, V.S.Y. Lin, M. Pruski, Conformations of silica-bound (pentafluorophenyl)propyl groups determined by solid-state NMR spectroscopy and theoretical calculations, J. Am. Chem. Soc. 132 (2010) 12452-12457.
[9] A.W. Overhauser, Polarization of nuclei in metals, Phys. Rev. 92 (1953) 411-415.
[10] T.R. Carver, C.P. Slichter, Polarization of nuclear spins in metals, Phys. Rev. 92 (1953) 212-213.
[11] R.A. Wind, Dynamic nuclear polarization, in Encyclopedia of NMR, eds. D.M. Grant, R.K. Harris, John Wiley, Chichester, 1996, 1798-1807.
[12] L.R. Becerra, G.J. Gerfen, B.F. Bellew, J.A. Bryant, D.A. Hall, S.J. Inati, R.T. Weber, S. Un, T.F. Prisner, A.E. McDermott, K.W. Fishbein, K.E. Kreischer, R.J. Temkin, D.J. Singel, R.G. Griffin, A spectrometer for dynamic nuclear-polarization and electron-paramagnetic-resonance at high-frequencies, J. Magn. Reson. Ser. A 117 (1995) 28-40.
[13] C.D. Joye, R.G. Griffin, M.K. Hornstein, K.-N. Hu, K.E. Kreischer, M. Rosay, M.A. Shapiro, J.R. Sirigiri, R.J. Temkin, P.P. Woskov, Operational characteristics of a 14-W 140-GHz gyrotron for dynamic nuclear polarization, IEEE Trans. Plasma Sci. 34 (2006) 518-523.
[14] M. Rosay, J.C. Lansing, K.C. Haddad, W.W. Bachovchin, J. Herzfeld, R.J. Temkin, R.G. Griffin, High-frequency dynamic nuclear polarization in MAS spectra of membrane and soluble proteins, J. Am. Chem. Soc. 125 (2003) 13626-13627.

[15] A.B. Barnes, M.L. Mak-Jurkauskas, Y. Matsuki, V.S. Bajaj, P.C.A. van der Wel, R. DeRocher, J. Bryant, J.R. Sirigiri, R.J. Temkin, J. Lugtenburg, J. Herzfeld, R.G. Griffin, Cryogenic sample exchange NMR probe for magic angle spinning dynamic nuclear polarization, J. Magn. Reson. 198 (2009) 261-270.
[16] E. Bouleau, P. Saint-Bonnet, F. Mentink-Vigier, H. Takahashi, J.F. Jacquot, M. Bardet, F. Aussenac, A. Purea, F. Engelke, S. Hediger, D. Lee, G. De Paepe, Pushing NMR sensitivity limits using dynamic nuclear polarization with closed-loop cryogenic helium sample spinning, Chem. Sci. (2015).
[17] K.-N. Hu, H.-h. Yu, T.M. Swager, R.G. Griffin, Dynamic nuclear polarization with biradicals, J. Am. Chem. Soc. 126 (2004) 10844-10845.
[18] C. Song, K.-N. Hu, C.-G. Joo, T.M. Swager, R.G. Griffin, Totapol: A biradical polarizing agent for dynamic nuclear polarization experiments in aqueous media, J. Am. Chem. Soc. 128 (2006) 11385-11390.
[19] Y. Matsuki, T. Maly, O. Ouari, H. Karoui, F. Le Moigne, E. Rizzato, S. Lyubenova, J. Herzfeld, T. Prisner, P. Tordo, R.G. Griffin, Dynamic nuclear polarization with a rigid biradical, Angew. Chem. Int. Ed. 48 (2009) 4996-5000.
[20] C. Sauvée, M. Rosay, G. Casano, F. Aussenac, R.T. Weber, O. Ouari, P. Tordo, Highly efficient, water-soluble polarizing agents for dynamic nuclear polarization at high frequency, Angew. Chem. Int. Ed. 52 (2013) 10858-10861.
[21] A. Zagdoun, G. Casano, O. Ouari, M. Schwarzwälder, A.J. Rossini, F. Aussenac, M. Yulikov, G. Jeschke, C. Copéret, A. Lesage, P. Tordo, L. Emsley, Large molecular weight nitroxide biradicals providing efficient dynamic nuclear polarization at temperatures up to 200 K, J. Am. Chem. Soc. 135 (2013) 12790-12797.
[22] T. Maly, G.T. Debelouchina, V.S. Bajaj, K.-N. Hu, C.-G. Joo, M.L. Mak-Jurkauskas, J.R. Sirigiri, P.C.A. van der Wel, J. Herzfeld, R.J. Temkin, R.G. Griffin, Dynamic nuclear polarization at high magnetic fields, J. Chem. Phys. 128 (2008) 052211.
[23] A. Lesage, M. Lelli, D. Gajan, M.A. Caporini, V. Vitzthum, P. Miéville, J. Alauzun, A. Roussey, C. Thieuleux, A. Mehdi, G. Bodenhausen, C. Copéret, L. Emsley, Surface enhanced NMR spectroscopy by dynamic nuclear polarization, J. Am. Chem. Soc. 132 (2010) 15459-15461.
[24] M. Lelli, D. Gajan, A. Lesage, M.A. Caporini, V. Vitzthum, P. Miéville, F. Héroguel, F. Rascón, A. Roussey, C. Thieuleux, M. Boualleg, L. Veyre, G. Bodenhausen, C. Copéret, L. Emsley, Fast characterization of functionalized silica materials by silicon-29 surface-enhanced NMR spectroscopy using dynamic nuclear polarization, J. Am. Chem. Soc. 133 (2011) 2104-2107.
[25] A.J. Rossini, A. Zagdoun, M. Lelli, J. Canivet, S. Aguado, O. Ouari, P. Tordo, M. Rosay, W.E. Maas, C. Copéret, D. Farrusseng, L. Emsley, A. Lesage, Dynamic nuclear polarization enhanced solid-state NMR spectroscopy of functionalized metal-organic frameworks, Angew. Chem. Int. Ed. 51 (2012) 123-127.
[26] A. Zagdoun, G. Casano, O. Ouari, G. Lapadula, A.J. Rossini, M. Lelli, M. Baffert, D. Gajan, L. Veyre, W.E. Maas, M. Rosay, R.T. Weber, C. Thieuleux, C. Copéret, A. Lesage, P. Tordo, L. Emsley, A slowly relaxing rigid biradical for efficient dynamic nuclear polarization surface-enhanced NMR spectroscopy: Expeditious characterization of functional group manipulation in hybrid materials, J. Am. Chem. Soc. 134 (2012) 2284-2291.

[27] T. Kobayashi, O. Lafon, A.S.L. Thankamony, I.I. Slowing, K. Kandel, D. Carnevale, V. Vitzthum, H. Vezin, J.-P. Amoureux, G. Bodenhausen, M. Pruski, Analysis of sensitivity enhancement by dynamic nuclear polarization in solid-state NMR: A case study of functionalized mesoporous materials, Phys. Chem. Chem. Phys. 15 (2013) 5553-5562.
[28] O. Lafon, A.S.L. Thankamony, T. Kobayashi, D. Carnevale, V. Vitzthum, I.I. Slowing, K. Kandel, H. Vezin, J.-P. Amoureux, G. Bodenhausen, M. Pruski, Mesoporous silica nanoparticles loaded with surfactant: Low temperature magic angle spinning C-13 and Si-29 NMR enhanced by dynamic nuclear polarization, J. Phys. Chem. C 117 (2013) 1375-1382.
[29] F.A. Perras, Z. Wang, P. Naik, I.I. Slowing, M. Pruski, Natural abundance 17O DNP sens provides 17O-1H distances with sub-picometer precision and insights into brønsted acidity, Angew. Chem. Int. Ed. (2017) DOI: 10.1002/anie.201704032.
[30] J.R. Yarava, S.R. Chaudhari, A.J. Rossini, A. Lesage, L. Emsley, Solvent suppression in DNP enhanced solid state NMR, J. Magn. Reson. 277 (2017) 149-153.
[31] D. Lee, S.R. Chaudhari, G. De Paepe, Solvent signal suppression for high-resolution MAS-DNP, J. Magn. Reson. 278 (2017) 60-66.
[32] A. Zagdoun, A.J. Rossini, D. Gajan, A. Bourdolle, O. Ouari, M. Rosay, W.E. Maas, P. Tordo, M. Lelli, L. Emsley, A. Lesage, C. Copéret, Non-aqueous solvents for DNP surface enhanced NMR spectroscopy, Chem. Commun. 48 (2012) 654-656.
[33] K.-N. Hu, V.S. Bajaj, M. Rosay, R.G. Griffin, High-frequency dynamic nuclear polarization using mixtures of tempo and trityl radicals, J. Chem. Phys. 126 (2007) 044512-044512.
[34] K.-N. Hu, C. Song, H.-H. Yu, T.M. Swager, R.G. Griffin, High-frequency dynamic nuclear polarization using biradicals: A multifrequency epr lineshape analysis, J. Chem. Phys. 128 (2008) 052302.
[35] F. Kurdzesau, B. van den Brandt, A. Comment, P. Hautle, S. Jannin, J.J. van der Klink, J.A. Konter, Dynamic nuclear polarization of small labelled molecules in frozen water-alcohol solutions, J. Phys. D (2008) 155506.
[36] U. Akbey, W.T. Franks, A. Linden, S. Lange, R.G. Griffin, B.-J. van Rossum, H. Oschkinat, Dynamic nuclear polarization of deuterated proteins, Angew. Chem. Int. Ed. 49 (2010) 7803-7806.
[37] D. Le, G. Casano, T.N.T. Phan, F. Ziarelli, O. Ouari, F. Aussenac, P. Thureau, G. Mollica, D. Gigmes, P. Tordo, S. Viel, Optimizing sample preparation methods for dynamic nuclear polarization solid-state NMR of synthetic polymers, Macromol. 47 (2014) 3909-3916.
[38] H. Takahashi, S. Hediger, G. De Paëpe, Matrix-free dynamic nuclear polarization enables solid-state NMR C-13-C-13 correlation spectroscopy of proteins at natural isotopic abundance, Chem. Commun. 49 (2013) 9479-9481.
[39] K. Kandel, S.M. Althaus, C. Peeraphatdit, T. Kobayashi, B.G. Trewyn, M. Pruski, Slowing, II, Substrate inhibition in the heterogeneous catalyzed aldol condensation: A mechanistic study of supported organocatalysts, J. Catal. 291 (2012) 63-68.
[40] J.H. Cavka, S. Jakobsen, U. Olsbye, N. Guillou, C. Lamberti, S. Bordiga, K.P. Lillerud, A new zirconium inorganic building brick forming metal organic frameworks with exceptional stability, J. Am. Chem. Soc. 130 (2008) 13850-13851.
[41] Z. Guo, T. Kobayashi, L.-L. Wang, T.W. Goh, C. Xiao, M.A. Caporini, M. Rosay, D.D. Johnson, M. Pruski, W. Huang, Selective host-guest interaction between metal ions and metal-organic frameworks using dynamic nuclear polarization enhanced solid-state NMR spectroscopy, Chem. Eur. J. 20 (2014) 16308-16313.

[42] D.P. Burum, W.K. Rhim, Improved NMR technique for homonuclear dipolar decoupling in solids - application to polycrystalline ice, J. Chem. Phys. 70 (1979) 3553-3554.
[43] D.R. Kinney, I.S. Chuang, G.E. Maciel, Water and the silica surface as studied by variable-temperature high-resolution H-1-NMR, J. Am. Chem. Soc. 115 (1993) 6786-6794.
[44] J. Trebosc, J.W. Wiench, S. Huh, V.S.Y. Lin, M. Pruski, Solid-state NMR study of MCM-41-type mesoporous silica nanoparticles, J. Am. Chem. Soc. 127 (2005) 3057-3068.
[45] A. Bielecki, A.C. Kolbert, M.H. Levitt, Frequency-switched pulse sequences - homonuclear decoupling and dilute spin NMR in solids, Chem. Phys. Lett. 155 (1989) 341-346.
[46] B.M. Fung, A.K. Khitrin, K. Ermolaev, An improved broadband decoupling sequence for liquid crystals and solids, J. Magn. Reson. 142 (2000) 97-101.
[47] S. Lange, A.H. Linden, U. Akbey, W.T. Franks, N.M. Loening, B.-J. van Rossum, H. Oschkinat, The effect of biradical concentration on the performance of DNP-MAS-NMR, J. Magn. Reson. 216 (2012) 209-212.
[48] F.A. Perras, A. Venkatesh, M.P. Hanrahan, T.W. Goh, W.Y. Huang, A.J. Rossini, M. Pruski, Indirect detection of infinite-speed MAS solid-state NMR spectra, J. Magn. Reson. 276 (2017) 95-102.
[49] S.R. Chaudhari, P. Berruyer, D. Gajan, C. Reiter, F. Engelke, D.L. Silverio, C. Coperet, M. Lelli, A. Lesage, L. Emsley, Dynamic nuclear polarization at 40 kHz magic angle spinning, Phys. Chem. Chem. Phys. 18 (2016) 10616-10622.